Environ. Eng. Res. Vol. 7, No. 3, pp. 137~148. 2002
Korean Society of Environmental Engineers

COLLOID MIGRATION IN A FRACTURED GRANITE: EVALUATION OF COLLOID MIGRATION PARAMETERS

Min-Hoon Baik†, Pil Soo Hahn, and Peter Vilks*

Korea Atomic Energy Research Institute

150 Dukjin-dong Yusong-gu, Daejeon 305-353, Korea

*Atomic Energy of Canada Limited, Pinawa, Manitoba, Canada R0E 1L0

(received February 2002, accepted July 2002)

Abstract : Colloid migration experiments using synthetic latex colloids of two different sizes in a fractured large granite block were carried out in order to understand the migration behaviors of colloids. A one-dimensional colloid migration model considering the filtration process was used in order to interpret the experimental results and to evaluate migration parameters of colloids such as average migration velocity, dispersion coefficient, and filtration coefficient. It was confirmed from our migration experiment that colloid can migrate faster than groundwater through a fractured rock. The average velocities and dispersion coefficients of all colloids were not overly dependent on the colloid sizes, but the filtration coefficients varied greatly with the sizes of colloids. It was observed that colloids with a relatively larger size could be filtered even in the fractured media although other processes can remobilize the filtered colloids.

Key Words : average migration velocity, colloid migration, dispersion coefficient, filtration coefficient, fractured rock

INTRODUCTION

In any consideration of the migration and dispersal of contaminants through saturated fractured and porous rock it is important to access the possible effects of colloids. Colloids (ultrafine particles usually less than 1 μm in diameter) may provide an alternative migration mechanism for radionuclides or toxic heavy metals. It has been reported that a formation of colloidal matter (true-colloid) or the sorption of a radionuclide on negatively charged naturally occurring colloidal matter (forming pseudo-colloid) could drastically increase the mobility of the radionuclides released from a radioactive waste repository.[1~3] The main result of the studies is that colloids can accelerate the migration of radionuclides in groundwater. Although many laboratory and field studies on the characteristics of natural colloids[4~11] and on the migration behaviors of colloidal particles in subsurface systems[12~20] have been performed, the mechanisms are not exactly known.

In fractures mobile colloids tend to stay within the center stream where the flow rate is highest (as in hydrodynamic chromatography experiments), and are subject to surface forces causing their motion relative to the fracture surfaces.[21] The transport nature of the colloids is also affected by the hydrodynamic interactions between the colloids, the groundwater,

†Corresponding author
E-mail: mhbaik@kaeri.re.kr
Tel: +82-42-868-2058

and the solid medium of the system. In addition, since the colloids are excluded from micropores in the rock matrix, the rock matrix diffusion and sorption as a retardation mechanism will be lessened.

Until now, only a few colloid migration experiments in a fractured medium have been carried out.[10,16,19] Thus, in this study, colloid migration experiments in a fractured granite block are carried out in order to understand the migration behaviors of colloids using synthetic latex colloids. A one-dimensional advective-dispersive colloid migration model considering the filtration process is used to interpret the experimental results and to estimate the migration parameters of colloids in a fractured rock.

EXPERIMENTAL

Preparation of the Granite Block

All migration experiments were performed in a natural fracture contained in a quarried block of granite, as shown in Figure 1. Granite block (called as LB-4), having dimensions of 83 × 90 × 60 cm, was obtained from the Whiteshell quarry near Whitemouth in Southeastern Manitoba, Canada.[16] The main fracture within the granite block dips about 9 degrees from a high, near boreholes BH-7 and BH-8, towards side CD.

Nine 3.8 cm diameter boreholes were drilled orthogonally from the surface of LB-4 until the main fracture was intersected. To maintain the water-saturated conditions and to avoid the inadvertent transport of fluid from the fracture into the interconnected pore space of the rock matrix as a result of drying out of the block, the granite block was saturated prior to performing migration experiments. After saturating the fractures and interconnecting pore spaces with groundwater, the granite block was coated with a siliconebased rubber compound to seal the outer surfaces. To further eliminate evaporative loss, LB-4 was immersed in a stainless steel tank containing groundwater.

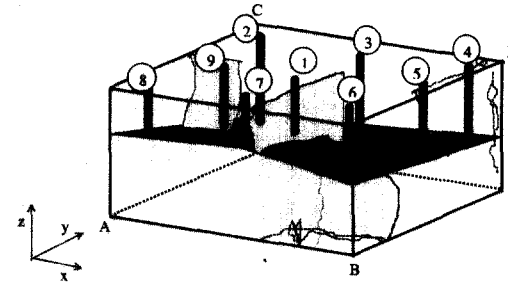

Figure 1. Schematic diagram of fractured large granite block (LB-4), showing main horizontal fracture, nine boreholes, and the orientations of the inferred vertical fractures.

The main fracture was accessed by stainless steel tubes, passing through the packers and rubber stoppers. Each stainless steel tube was fitted with a valve, allowing a flow path to be established in the main fracture between any combinations of boreholes. The combined water volume in the stainless steel tubes used for injection and recovery was about 2 mL, which represented 1 to 2 percent of the flow path volume.

Hydraulic Characterization of the Fracture

Initially the granite block LB-4 was hydraulically tested after being relocated to the fume hood. This was intended to provide basic hydraulic information for the fracture, and was used to help in deciding which boreholes to use for the migration tests. The initial tests were performed without the addition of colloids to evaluate the migration behavior of dissolved tracers alone.

The hydraulic transmissivity of the fracture between a pair of boreholes was determined from the hydraulic head difference required to maintain a constant flow of about 384 mL/min through the fracture between the two boreholes. A water manometer, which was connected to the inlet borehole, was used to measure the hydraulic head difference required to maintain the flow rate. Based on the information obtained from the hydraulic characterization, boreholes BH-6 and BH-9 were selected as the

inlet and outlet boreholes, respectively.

Method

All migration experiments were carried out with a dipole flow field established by injecting into borehole BH-6 with a high performance liquid chromatography (HPLC) syringe pump at a rate of 15 mL/h, and collecting water from borehole BH-9 with a fraction collector. The groundwater taken from underground borehole HC-12 located in fracture zone 2 (FZ-2) of the URL (Underground Research Laboratory), Manitoba, Canada was used as a carrier solution.[11]

Synthetic fluorescent latex colloids (Interfacial Dynamics Co.) of two different sizes were used as colloid tracers. The polystyrene latex colloids which have fluorescent dye colors consisted of blue latex colloids with a size of 1.0 μm and red latex colloids with a size of 0.2 μm. Bromide (Br^- as KBr) was also used as a conservative tracer in order to simulate the groundwater flow in the fracture.

The experimental set-up for colloid migration in LB-4 for a selected flow path (i.e., from the boreholes BH-6 to BH-9) is shown in Figure 2. The tracer injection was initiated by turning valves to redirect groundwater from the HPLC pump into an accumulator, containing the mixture of tracers, and forcing the tracers into the borehole BH-6. This was considered as time zero for all tracer tests and initiated sample collection. After 5 hours, giving a total injected volume of 75 mL, the tracer injection was terminated and tracer-free groundwater was redirected back to borehole BH-6.

Total colloid concentrations in eluted groundwater were determined by a Spectrofluorometer. The concentration of the bromide was determined by an ion chromatography. Summary of the migration experiments is given in Table 1.

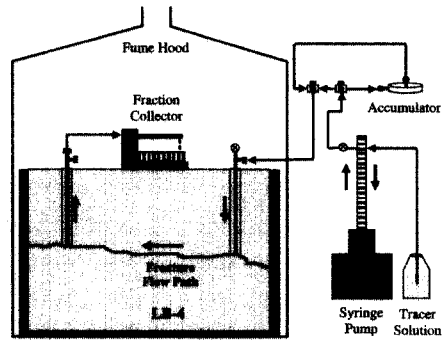

Figure 2. Experimental set-up scheme for radionuclide migration in LB-4.

Table 1. Summary of colloid migration experiments

Tracers	Concentrations	First arrival time (h)	Peak arrival time (h)	Percent total recovery
Br^-	1,070 mg/L	10.1	22.3	100
Blue latex colloids (1.0 μm)	6.76×10^7	8.7	14.7	5.4
Red latex colloids (0.2 μm)	1.81×10^{12} particles/mL	10.0	17.3	100

COLLOID MIGRATION MODEL

A discrete representation of rock fractures has been widely used in the problem of groundwater flow and solute transport. In this case, each fracture is represented by a pair of parallel plates with a constant aperture width based upon an advective-dispersive migration model. The advective-dispersive migration model describes solute transport by a mean velocity and Fickian-type variation of the residence times around the mean. This has been shown to be a good description of the solute transport in fractured media as well as in homogeneous porous media.

Thus, in this study, a colloid migration model based upon the advective-dispersive model is used to elucidate and analyze the results of colloid migration experiments. To model colloid migration, three assumptions are to be introduced:

(1) advective-dispersive transport can also be applied to colloid migration,
(2) colloids are too large to diffuse into the rock matrix, and
(3) mono-disperse colloids are considered.

Based on these assumptions, the following processes are considered for the formulation of

the colloid migration equation:

(1) advection of colloids along the fracture,
(2) longitudinal dispersion of colloids in the fracture,
(3) sorption of colloids onto the surface of the fracture, and
(4) filtration of colloids through the fracture.

Due to the assumption that the colloids do not diffuse into the porous rock matrix, the migration equation for mono-disperse colloids in the fracture can thus be given as:

$$\frac{\partial C_{fc}}{\partial t} + \frac{2}{b}\frac{\partial S_{fc}}{\partial t} + \frac{\partial \sigma_{fc}}{\partial t} = \frac{\partial}{\partial x}\left(D_{fc}\frac{\partial C_{fc}}{\partial x}\right) - V_{fc}\frac{\partial C_{fc}}{\partial x} \quad (1)$$

Here C_{fc} is defined as the mass of mobile colloids in solution per unit volume of solution in the fracture, S_{fc} as the mass of sorbed colloids onto the fracture surface per unit area of the fracture surface, and σ_{fc} as the mass of colloids filtered per unit volume of the fracture.

When colloidal particles are small enough to enter a porous medium and are deposited at different locations within the porous medium the process is called deep-bed filtration.[22] Deep-bed filtration is usually observed in large open fractures or unconsolidated porous media when the size of the colloidal particles is smaller than a characteristic fracture aperture or pore diameter.[15] Many deep-bed filtration models have been proposed in order to examine the properties of colloid migration in porous media.[22,23] In fractured porous media, a less capture of colloids is observed than in unfractured porous media due to the larger flow channels and less tortuous pathways in the fractures.[13] In this study, we considered the filtration of colloids in the fracture since micro-fissures or micro-pores are usually present on the fracture surfaces and fracture filling materials exist in the fracture.

For the filtration process, the following equation, originally proposed by several researchers for porous media applications,[22] is used to describe the change in the concentration of the filtered colloids over time in a fracture:

$$\frac{\partial \sigma_{fc}}{\partial t} = \lambda_{fc} V_{fc} C_{fc} \quad (2)$$

where λ_{fc} is defined as the filtration coefficient and the rate of colloid filtration is described by $\lambda_{fc} V_{fc}$. In Eq. (2), it is assumed that the filtration process is unlimited and that the remobilization of filtered colloids is neglected. The remobilization of filtered colloids during transport has been reported,[22] and its neglect leads to an underestimation of the migration of colloids.

Several investigators suggested that a simplified linear sorption model could be used for colloid migration, conservatively.[24] Thus, the sorption of colloids onto the fracture surfaces are given by using the concept of distribution coefficient as:

$$S_{fc} = K_{ac} C_{fc} \quad (3)$$

Therefore, a governing equation for the colloid migrating in the fracture can be given by inserting Eqs. (2) and (3) into Eq. (1):

$$R_{ac}\frac{\partial C_{fc}}{\partial t} = \frac{\partial}{\partial x}\left(D_{fc}\frac{\partial C_{fc}}{\partial x}\right) - V_{fc}\frac{\partial C_{fc}}{\partial x} - \lambda_{fc} V_{fc} C_{fc} \quad (4)$$

where R_{ac} is the retardation factor of the colloid in the fracture and defined as:

$$R_{ac} = 1 + \frac{2}{b} K_{ac} \quad (5)$$

In order to solve the governing equation, first of all, zero initial and step input conditions are considered. Thus the initial condition for the colloid migration equation is given as:

$$C_{fc}(x, 0) = 0 \quad (6)$$

If the colloid tracer is introduced at time t_i

at the inlet with a constant concentration of C_{c0}, the response elution curve can be obtained, i.e.,

$$C_{fc}(0,\ t) = C_{c0} \quad \text{if} \quad t \geq t_i \tag{7a}$$

$$C_{fc}(0,\ t) = 0 \quad \text{if} \quad t < t_i \tag{7b}$$

Also the infinite output boundary condition is used:

$$C_{fc}(\infty, t) = 0 \tag{8}$$

Subjecting to the initial and boundary conditions, the analytical solution of the governing equation at the concentration outlet at a distance L along the fracture, can be written as:[25]

$$\frac{C_{fc}(L,t)}{C_{c0}} = \frac{1}{2}\left[exp\left(\frac{Pe^c(1-\beta)}{2}\right) \cdot erfc\left(\frac{1-\beta\frac{t}{t_{oc}}}{2\sqrt{\frac{t}{Y}}}\right) + exp\left(\frac{Pe^c(1+\beta)}{2}\right) \cdot erfc\left(\frac{1+\beta\frac{1}{t_{oc}}}{2\sqrt{\frac{t}{Y}}}\right)\right] \tag{9}$$

where

$$Pe^c = \frac{V_{fc} \cdot L}{D_{fc}} \tag{10}$$

$$t_{oc} = \frac{R_{ac} \cdot L}{V_{fc}} \tag{11}$$

$$Y = Pe^c \cdot t_{oc} \tag{12}$$

$$\beta^2 = 1 + \frac{4\lambda_{fc} R_{ac} L}{Pe^c} \tag{13}$$

The dimensionless Peclet number of the colloid, Pe^c, represents the relative importance of longitudinal dispersion compared with the advective flow of colloids by its own definition.[25]

In this study, however, a finite rectangular pulse input with constant time duration was used in all colloid migration experiments. Thus the analytical solution, Eq. (9), should be modified in order to consider the finite rectangular pulse input. Consequently, the final analytical solution of the governing equation at the outlet, L, can be written as:

$$C_{fc}^{rec}(L,t) = C_{fc}(L,t)U(t) - C_{fc}(L, t-t_i)U(t-t_i) \tag{14}$$

where C_{fc}^{rec} is the analytical solution obtained for the case of the rectangular pulse input and and $U(t)$ is the step function with

$$U(t) = 1 \quad \text{for} \quad t \geq 0 \tag{15a}$$

$$U(t) = 0 \quad \text{for} \quad t < 0 \tag{15b}$$

RESULTS AND DISCUSSION

Experimental Results

The results of the migration experiments are illustrated as elution profiles in Figures 3 to 5 for bromide, blue latex colloid (1.0 μm), and red latex colloid (0.2 μm), respectively. The tracer concentrations eluted are plotted as C/C_0 versus elution time. Summary of the elution profiles for the migration experiments is given in Table 1, which gives the times for the first tracer arrival and the peak arrival, and the total percent of recovery.

A comparison of tracer recoveries is a useful indicator of a tracer's ability to migrate within the fracture. Mass loss processes like rock matrix diffusion and filtration through fractures may reduce the ability of a tracer to migrate within the fracture. The total recoveries of Br^- and red latex colloids are about 100%, thus all Br^- and red latex colloids are recovered. The total recovery of the blue latex colloids is significantly less than those of Br^- and red latex colloids. It can therefore be concluded that the ability of colloids to migrate though the fracture is not reduced for the relatively smaller colloids although the ability of colloids to migrate can be reduced for the relatively larger colloids.

When compared to the case of the conservative tracer (Br^-), the arrival time is a useful

indicator of whether a tracer is retarded by sorption, or whether it is traveling along a more direct flow path than the average water mass. This may occur in the case of colloid migration. Although blue latex colloids have the lowest recovery, they have faster arrival times than Br^- and red latex colloids. The first arrival time of the red latex colloids is similar to Br^-. This faster migration of the blue latex colloids may be due to the hydrodynamic and size exclusion effects.[21]

In a smooth-walled fracture it is known that the velocity profile for a flowing Newtonian fluid takes on a parabolic shape in which the maximum velocity occurs at the center of the fracture. When colloidal particles are suspended in the fluid, colloids are dispersed normal to the direction of flow by Brownian motion, and these colloids travel at various velocities across the width of the fracture. Larger particles are, because of their size, excluded from the slowest groundwater velocity zone near the fracture wall and, as a result, tend to move faster than smaller particles.[21]

Model Calculations and Fittings

The hydraulic transmissivity within the fracture in the selected flow pathway was determined by:[26]

$$T_r = \frac{Q}{2\pi \triangle h} \ln\left(\frac{r_w}{L}\right) \tag{16}$$

Using Darcy's law and cubic law, the average aperture width of a fracture between the two plates can be given as:[26]

$$\bar{b} = \left(\frac{12\mu T_r}{\rho_w g}\right)^{1/3} \tag{17}$$

In our experimental system, the hydraulic head ($\triangle h$) was measured as 0.1 cm and thus the transmissivity (T_r) and mean fracture aperture ($\bar{b}$) were calculated as 1.11967 cm^2/s and 0.05162 cm, respectively, using the data listed in Table 2.

The results of the colloid migration experiments are fitted using the colloid migration model in order to obtain the parameters such as Peclet number, residence time, and filtration coefficient. Model fitting curves for the experimentally obtained elution profiles are also shown in Figures 3 to 5 for bromides, blue latex colloids, and red latex colloids, respectively. The values of the parameters used in the model calculations are listed in Table 2.

As shown in Figures 3 and 4, the predicted profiles for bromide and blue latex colloids are well fitted with the experimental elution profiles. For red latex colloids, as shown in Figure 5, the calculated fitting curve agrees with the experimental data with the exception at the tail of the fitting curve. The discrepancy around the tail between the calculated fitting curve and experimental data may be due to

Table 2. Values of the parameters used in model calculations

Parameter	Definition	Dimension	Value	Reference
Porosity	θ	-	0.03	29
Linear migration length	L	cm	76.1	*
Density of rock	ρ_b	g/cm^3	2.643	26
Rock matrix diffusion coefficient of Br	D_{pr}	cm^2/s	1.0×10^{-9}	26
Flow rate	Q	mL/s	0.25	*
Hydraulic head difference	$\triangle h$	cm	0.1	*
Transmissivity	T_r	cm^2/s	1.11967	*
Mean fracture aperture	$\bar{b}$	cm	0.05162	*
The radius of injection and withdrawal boreholes	r_w	cm	0.104	*
Distribution coefficient of all colloids	K_{ac}	cm^3/g	0	assumed

*values obtained in this study

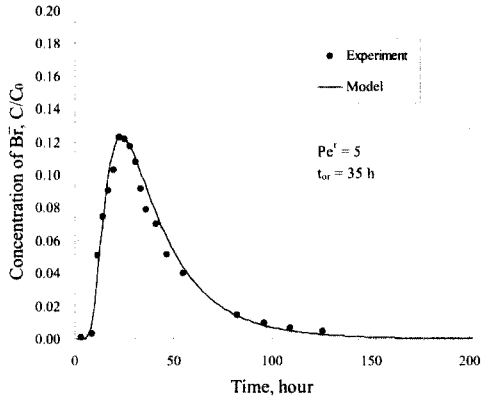

Figure 3. Model fitting result for the conservative tracer Br^- migration in the LB-4.

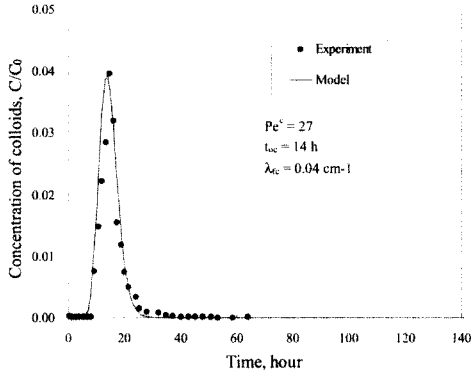

Figure 4. Model fitting result for the blue latex colloids migration in the LB-4.

several factors. One is an experimental error in the concentration measurement of the red latex colloids and another reason may be due to the uncertain dispersion mechanisms. It has been difficult to identify and quantify how much of the observed discrepancy is the result of the dispersive mechanisms or of incomplete recovery of the tracer.

Table 3 summarizes the Peclet number and residence time of bromides and colloids, which were obtained by the model fittings. However, the filtration coefficient was obtained by the parameter evaluation using the total percent of recovery, i.e., Eq. (27). It is shown that the residence time (t_{oc}) and Peclet number (Pe^c) of the colloids are not greatly dependent upon the sizes of the colloids, but the filtration

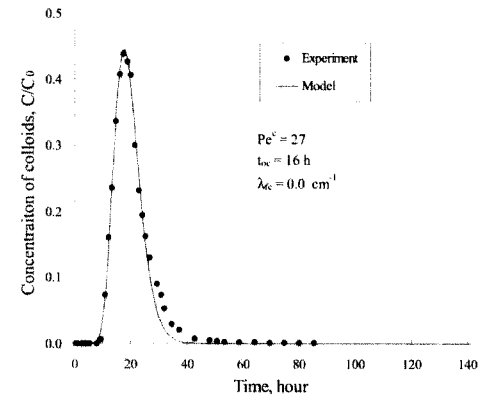

Figure 5. Model fitting result for the red latex colloids migration in the LB-4.

Table 3. Migration parameters of bromide and colloids obtained by model fittings to experimental data

Tracers	Residence time t_{or} or t_{oc} (h)	Peclet number Pe^r or Pe^c	Filtration coefficient λ_{fc}(1/cm)
Br^-	35	5	0
Blue latex colloids (1.0 μm)	14	27	0.04
Red latex colloids (0.2 μm)	16	27	0

coefficient (λ_{fc}) greatly depends on the sizes of the colloids. Thus it is concluded that the filtration of colloids within the fracture greatly depends on the size of colloids and the filtration may not be occurred when the size of colloids is small.

Evaluation of Colloid Migration Parameters

Average migration velocity : The average velocities of colloids can be calculated using the definition of the residence time of the colloid, which is obtained by the model fitting:

$$V_{fc} = L/t_{oc} \tag{18}$$

Calculated results are listed in Table 4. The calculated results show that all colloids have almost the same V_{fc} since all colloids have similar residence times and that the average velocities of colloids are not greatly dependent upon the colloid sizes.

Table 4. Model calculated and data fitted migration parameters of colloids

Tracers	ϕ_c (μm)	V_{fc} (cm/s)	D_{fc} (cm^2/s)	D_{Bfc} (cm^2/s)	α_{fc} (cm)	λ_{fc} (1/cm)
Blue latex colloids	1.0	1.51×10^{-3}	4.26×10^{-3}	2.15×10^{-10}	2.82	0.04
Red latex colloids	0.2	1.32×10^{-3}	3.72×10^{-3}	4.29×10^{-9}	2.82	0

On the other hand, the average groundwater velocity can be obtained by using the data from Br^-, i.e., $V_w=L/t_{or}=6.04\times10^{-4}$ cm/s. By comparing V_{fc} with V_w, it is apparent that the average colloid velocity is much greater than that of the groundwater as we discussed previously.

Dispersion coefficient : The dispersion coefficients of colloids can be obtained by using the definition of Peclet number described in Eq. (10) as:

$$D_{fc}=\frac{V_{fc}\cdot L}{Pe^c} \tag{20}$$

The dispersion coefficients of the colloids calculated by the Eq. (20) are given in Table 4. The hydrodynamic dispersion coefficient of bromide can be calculated using an equation similar to Eq. (20), i.e., $D_{fr}=V_{fr}\cdot L/Pe^r=5.75\times10^{-3}$ cm^2/s.

Dispersion of a solute in a single, uniform, parallel-walled fracture is described by Taylor's dispersion theory, which has recently been applied to the dispersion of radionuclides sorbed on colloids.[14] Generally, in the case of uniform flow and isotropic medium, the hydrodynamic dispersion coefficient for the dissolved species, D_{fr}, is generally expressed as:[27]

$$D_{fr}=D_r^*+\alpha_{fr}V_{fr} \tag{21}$$

Similarly, the hydrodynamic dispersion coefficient of a colloid with a diameter of ϕ_c can be also expressed as:[17]

$$D_{fc}=D_{Bfc}+\alpha_{fc}V_{fc} \tag{22}$$

The diffusivity of colloids is different from that of truly dissolved species, which gives rise to different dispersivity since the Brownian diffusion coefficient for colloids is not necessarily equal to the molecular diffusion coefficient of the dissolved species.

The Brownian diffusion coefficient of colloids in the fracture can be usually given by the Stokes-Einstein relation:[17]

$$D_{Bfc}=\frac{k_BT}{3\pi\mu\phi_c} \tag{23}$$

The diffusion coefficients of the major ions in groundwater are generally in the range of 1×10^{-5} to 2×10^{-5} cm^2/s at 25℃.[27] In this study, D_r^* is assumed to be 1×10^{-5} cm^2/s. In order to estimate the dispersivity of the bromide and colloids, α_{fr} and α_{fc}, we used the fitted values of the parameters. Thus, using Eqs. (21) and (22), α_{fr} and α_{fc} can be expressed as:

$$\alpha_{fr}=\frac{D_{fr}-D_r^*}{V_{fr}}=\frac{L}{Pe^r}-\frac{D_r^*}{V_{fr}}=15.2 \tag{24}$$

and

$$\alpha_{fc}=\frac{D_{fc}-D_{Bfc}}{V_{fc}}=\frac{D_{fc}-D_{Bfc}}{V_{fc}}=\frac{L}{Pe^c}-\frac{D_{Bfc}}{V_{fc}} \tag{25}$$

The calculated dispersivities of the colloids are also presented in Table 4. Dispersion is believed to be dominated by the differing transit times through the fracture network and therefore α_{fc} is a function of the fracture network geometry only, and does not depend on the smaller scale mechanisms determining dispersion in single fractures. Therefore, in general, α_{fc} is assumed to be independent colloid size and is assigned the same values for dissolved species and colloids, i.e., $\alpha_{fc}\cong\alpha_{fr}$.

However, as shown in Table 4, α_{fc} is actually not the same as α_{fr} but rather α_{fc} is smaller than α_{fr}. This result may be more relevant than the assumption of $\alpha_{fc} \cong \alpha_{fr}$.

Filtration coefficient : As observed in the results of colloid migration in LB-4, the recoveries of the blue latex colloids with diameter of 1.0 μm were much less than 100%. The loss of colloids through the fracture can be due to such processes as filtration, gravitational settling, and diffusion to stagnant zones.

A possibility of the colloid loss due to the gravitational settling can be investigated by a simple calculation procedure. The gravitational settling velocity of a colloid can be calculated using Stokes' law:

$$V_s = \frac{\phi_c^2(\rho_c - \rho_w)g}{18\mu} \tag{26}$$

The calculated V_s is about 10^{-6} cm/s for the blue latex colloids. Since the settling velocity of the migrating blue latex colloids is much less than the groundwater velocity, the settling of the migrating blue latex colloids is hard to occur within the fracture. In the present study, therefore, the loss of the blue latex colloids was considered to be due to the filtration of the colloids through the fracture.

The filtration coefficient is typically an empirically determined coefficient, which expresses the efficiency of a medium in filtering colloidal particles from suspensions. It usually varies with colloid size and species.[12] Unfortunately, experimental values of the filtration coefficient for a single fracture are not available in literatures, although many filtration coefficient values have been estimated for nonfractured porous media.[22]

The filtration coefficient can be estimated by using the recoveries of colloids in elution data assuming that the loss of colloids through fracture is only due to the filtration process:[28]

$$\lambda_{fc}^m = \ln\left(\frac{100}{\%\ of\ elution}\right)/L \tag{27}$$

Table 4 shows the filtration coefficients for the two different colloids, which are obtained by Eq. (27). As shown in Table 4, no filtration was occurred for the red latex colloids with diameter of 0.2 μm. The values of the filtration coefficient for the blue latex colloids is about 0.04 cm^{-1} and this value is very similar to the values of the filtration coefficients of the same blue latex colloids observed in a porous granite column.[18] Thus it is noticed that the filtration coefficient greatly depends on the size of the colloid and no filtration occurs in the fracture when the size of colloids is small.

CONCLUSIONS

In this study, colloid migration experiments in a fractured large granite block were carried out in order to understand the migration behaviors of colloids. A one-dimensional colloid migration model considering the filtration process was used and calculated in order to interpret the experimental results and to evaluate migration parameters of colloids such as average migration velocity, dispersion coefficient, and filtration coefficient.

From the experimental and model study, the following conclusions were made:

1. The average colloid velocity is much greater than that of the groundwater in the fracture. The recoveries of colloids are significantly less than that of the conservative tracer when the size of colloids is large and decrease with increasing colloidal size.
2. The average velocities and dispersion coefficients of all colloids are not overly dependent on the colloid sizes, but the filtration coefficients greatly depend upon the sizes of colloids.
3. The filtration process of colloids can be important not only in porous media but also in fractured media when the size of colloids is large. However, it should be reminded that the filtered colloids can be remobilized and then the migration of colloids could be more pronounced.

ACKNOWLEDGEMENT

This study was supported by the Nuclear R&D Program of Ministry of Science and Technology, Korea.

NOMENCLATURES

$\bar{b}$ average width of the fracture aperture, cm

C_{c0} initial concentration of colloids injected, g/cm^3

C_{fc} mobile colloid concentration in the fracture, g/cm^3

C_{fc}^{rec} mobile colloid concentration in the fracture obtained for the case of the rectangular pulse input defined in Eq. (14), g/cm^3

D_{Bfc} Brownian diffusion coefficient of colloids in the fracture, cm^2/s

D_{fc} dispersion coefficient of mobile colloids in the fracture, cm^2/s

D_{fr} dispersion coefficient for the conservative tracer Br$^-$, cm^2/s

D_r^* molecular diffusion coefficient of the conservative tracer Br$^-$ in the water, cm^2/s

g gravitational acceleration, cm/s^2

k_B Boltzmann constant, dyne/K

K_{ac} distribution coefficient of the colloids between the aqueous solution and fracture surface defined in Eq. (3), cm

L length of flow path in the fracture, cm

Pe^c Peclet number of the colloid defined in Eq. (10)

Pe^r Peclet number of the conservative tracer Br$^-$

Q solution flow rate, cm^3/s

r_w radius of injection and withdrawal boreholes, cm

R_{ac} fracture surface retardation factor of the colloid defined in Eq. (5)

S_{fc} immobile colloid concentration sorbed onto fracture surfaces, g/cm^2

t time, s

T_r transmissivity of the fracture defined in Eq. (16), cm^2/s

T absolute temperature of water, K

t_i time when a tracer is injected, s

t_{oc} residence time of the colloid in the fracture, s

t_{or} residence time of the conservative tracer Br$^-$ in the fracture, s

$U(t)$ unit step function defined in Eq. (15)

V_{fc} average velocity of the mobile colloids in the fracture, cm/s

V_w average velocity of the groundwater in the fracture, cm/s

V_s settling velocity of the colloids, cm/s

x distance along the fracture, cm

α_{fr} dispersivity of the conservative tracer Br$^-$ in the direction of the fracture axis, cm

α_{fc} dispersivity of the colloids in the direction of the fracture axis, cm

Δh hydraulic head difference, cm

ϕ_c diameter of the mono-disperse colloids, cm

λ_{fc} filtration coefficient of the colloids through the fracture defined in Eq. (2), 1/cm

μ viscosity of the groundwater, g/cm · s

ρ_w density of the groundwater, g/cm^3

ρ_c density of the colloids, g/cm^3

σ_{fc} immobile colloid concentration filtered through the fracture, g/cm^3

REFERENCES

1. Avogadro, A. and De Masily, G., "The role of colloids in nuclear waste disposal," *Mater. Res. Soc. Symp. Proc.*, **26**, 495 (1984).
2. Kim, J. I., Buckau, G., Baumgartner, F., Moon, H. C., and Lux, D., "Colloid generation and the actinide migration in groundwaters," *Mater. Res. Soc. Symp. Proc.*, **26**, 31~40 (1984).
3. Neretnieks, I., Some aspects on colloids as a means for transporting radionuclides,

KBS/TR-103, Swedish Nuclear Fuel and Waste Management Co., Stockholm (1978).
4. Vilks, P., Cramer, J. J., Schewchuck, T. A., and Larocque, J. P. A., "Colloid and particulate matter studies in the Cigar Lake Natural-Analog Program," *Radiochim. Acta*, **44/45**, 305~310 (1988).
5. Orlandini, K. A., Penrose, W. R., Harvey, B. R., Lovett, M. B., and Findlay, M. W., "Colloidal behavior of actinides in an Oligotrophic lake," *Environ. Sci. Technol.*, **24**, 706~712 (1990).
6. Vilks, P. and Degueldre, C., "Sorption behaviour of ^{85}Sr, ^{131}I, ^{137}Cs on colloids and suspended particles from the Grimsel Test Site, Switzerland," *Appl. Geochem.*, **6**, 553~563 (1991).
7. Vilks, P., Miller, H. G., and Doern, D. C., "Natural colloids and suspended particles in the Whiteshell Research area, Manitoba, Canada, and their potential effect on radiocolloid formation," *Appl. Geochem.*, **6**, 565~574 (1991).
8. Allard, B., Karlsson, F., and Neretnieks, I., Concentration of particulate matter and humic substances in deep groundwaters and estimated effects on the adsorption and transport of radionuclides, SKB/TR 91-50, Swedish Nuclear Fuel and Waste Management Co., Stockholm (1991).
9. Degueldre, C., "Colloid properties in granitic groundwater systems with emphasis on the impact on safety assessment of a radioactive waste repository," *Mater. Res. Soc. Symp. Proc.*, **294**, 817~823 (1993).
10. McKay, L. D., Gillham, R. W., and Cherry, J. A., "Field experiments in a fractured clay till. 2. Solute and colloid transport," *Water Resour. Res.*, **29**, 3879~3890 (1993).
11. Baik, M. H., Hahn, P. S., and Vilks, P., Characterization of natural colloids sampled from deep granite groundwater of the Canadian Shield, *Environ. Eng. Res.*, **4**(3), 165~176 (1999).
12. Satelli, A., Avogadro, A., and Bidoglio, G., "Americium filtration in glauconitic sand columns," *Nucl. Technol.*, **67**, 245~254 (1984).
13. Toran L. and Palumbo, A. V., "Colloid transport though fractured and unfractured laboratory sand columns," *J. Cont. Hydrol.*, **9**, 289~303 (1992).
14. Smith, P. A. and Degueldre, C., "Colloid-facilitated transport of radionuclides through fractured media," *J. of Cont. Hydrol.*, **13**, 143~166 (1993).
15. Ibaraki, M. and Sudicky, E. A., "Colloid-facilitated contaminant transport in discretely fractured porous media 1. Numerical formulation and sensitivity analysis," *Water Resour. Res.*, **31**(12), 2945~2960 (1995).
16. Vilks, P. and Bachinski, D. B., "Colloid and suspended particle migration experiments in a granite fracture," *J. Cont. Hydrol.*, **21**, 269~279 (1996).
17. Baik, M. H. and Hahn, P. S., "Radionuclide transport facilitated by polydispersed pseudo-colloids in the fractured rock media," *J. Nucl. Sci. Technol.*, **34**(1), 41~49 (1997).
18. Cho, H. K., Baik, M. H., and Choi, H. S., "Experimental study on the colloid migration phenomena through crushed granite columns," *J. Korean Soc. Environ. Eng.*, **23**(2), 281~292 (2001).
19. Vilks, P. and Baik, M. H., "Laboratory Migration experiments with radionuclides and natural colloids in a granite fracture," *J. Cont. Hydrol.*, **47**, 197~210 (2001).
20. Contard J. S., Turner, D. R., and Ahn, T. M., "Modeling colloid transport for performance assessment," *J. Cont. Hydrol.*, **47**, 323~333 (2001).
21. Small, H., "Hydrodynamic chromatography: A technique for size analysis of colloidal particles," *J. Coll. Inter. Sci.*, **48**, 147~161 (1974).
22. Herzig, J. P., Leclerc, D. M., and Le Goff, P., "Flow of suspensions through porous media: Application to deep filtration," *Ind. Eng. Chem.*, **62**, 8~35 (1970).
23. Tien, C. and Payatakes, A. C., "Advances in deep-bed filtration," *AIChE J.*, **25**, 737~759 (1979).

24. Ticknor, K. V., Vilks, P., and Vandergraaf, T. T., The effect of fulvic acid on contaminant sorption by granite and selected minerals, AECL TR-669, Atomic Energy of Canada Limited, Pinawa (1995).
25. Bear, J., Dynamics of Fluids in Porous Media, American Elsevier, New York (1972).
26. Vandergraaf, T. T. and Drew, D. J., "Laboratory studies of radionuclide transport in fractured crystalline rock," *Proceedings of 3rd International Symposium on Advanced Nuclear Energy Research-Global Environment and Nuclear Energy*, March 13-15, Minto City, Japan, pp. 385~393 (1991).
27. Freeze, R. A. and Cherry, J. A., Groundwater, Prentice-Hall Inc., Englewood Cliffs (1972).
28. Tipping, E., Thompson, D. W., Woaf, C., and Longworth, G., Transport of haematite and silica colloids through sand column eluted with artificial groundwater, Harwell Laboratory (1991).
29. Wels, C., Smith, L., and Vandergraaf, T. T., "Influence of specific surface area on transport of sorbing solutes in fractures: An experimental analysis," *Water Resour. Res.*, **32**, 1943~1954 (1996).